BIOCHEMISTRY
including biophysical chemistry & molecular biology
Article

Biochemistry **2010,** *49,* 3009–3023 3009
DOI: 10.1021/bi901523y

Replication of a Universal Nucleobase Provides Unique Insight into the Role of Entropy during DNA Polymerization and Pyrophosphorolysis†

Xuemei Zhang,‡ Edward Motea,§ Irene Lee,§ and Anthony J. Berdis*,‡

‡*Department of Pharmacology and* §*Department of Chemistry, Case Western Reserve University, 10900 Euclid Avenue, Cleveland, Ohio 44106*

Received August 31, 2009; Revised Manuscript Received February 2, 2010

ABSTRACT: Most models accounting for the efficiency and fidelity of DNA polymerization invoke the use of either hydrogen bonding contacts or complementarity of shape and size between the formed base pair. This report evaluates these mechanisms by quantifying the ability of a high-fidelity DNA polymerase to replicate 5-nitroindole, a purine mimetic devoid of classic hydrogen bonding capabilities. 5-NITP acts as a universal nucleotide since it is incorporated opposite any of the four natural nucleobases with nearly equal efficiencies. Surprising, the polymerization reaction is not reciprocal as natural nucleotides are poorly incorporated opposite 5-nitroindole in the template strand. Incorporation opposite 5-nitroindole is more efficient using natural nucleotides containing various modifications that increase their base stacking potential. However, 5-substituted indolyl nucleotides that contain π-electron and/or hydrophobic groups are incorporated opposite the non-natural nucleobase with the highest catalytic efficiencies. The collective data set indicate that replication of a non-natural nucleobase is driven by a combination of the hydrophobic nature and π-electron surface area of the incoming nucleotide. In this mechanism, the overall hydrophobicity of the incoming nucleobase overcomes the lack of hydrogen bonding groups that are generally required for optimal DNA polymerization. However, the lack of hydrogen bonds between base pairs prevents primer extension. This final aspect is manifest by the appearance of unusually high pyrophosphorolysis activity by the T4 DNA polymerase that is only observed with the non-natural nucleobase in the template. These results highlight the importance of hydrogen bonding interactions during primer extension and pyrophosphorolysis.

DNA polymerases catalyze the addition of mononucleotides to a growing polymer using a DNA template as a guide for each incorporation event. The efficiency and fidelity of DNA polymerization have historically been attributed to enthalpic contributions caused by the formation of proper Watson−Crick base pairs between the incoming nucleotide and the corresponding templating base (*1*, *2*). Early studies comparing the kinetics of correct versus incorrect nucleotide incorporation (*3*−*6*) have led to a fundamental model for how DNA polymerases maintain genomic fidelity. In this model, DNA polymerases simply "read" the coding information present within the hydrogen bonds of the template nucleobase. In fact, the mutual recognition of adenine (A) by thymine (T) and of guanine (G) by cytosine (C) involves the formation of complementary hydrogen bonds between the functional groups of each pair. Furthermore, the lack of hydrogen bonding compatibility between A and C, for example, would hinder the polymerase's ability to form such base pairs and, thus, maintain genomic fidelity.

Despite the intuitive nature of this model, there is a growing body of evidence that a simple mechanism invoking hydrogen bonding interactions is incomplete. A compelling argument against the reliance of hydrogen bonds comes from the ability of various DNA polymerases to efficiently utilize nucleotide analogues devoid of classical hydrogen bonding functional groups (*7*). One of the earliest examples of this phenomenon is the ability of the *Escherichia coli* Klenow fragment to effectively incorporate dAMP[1] opposite 2,4-difluorotoluene (dF), an isostere of thymine that lacks functional groups associated with hydrogen bonding (*8*, *9*). In addition, the replication of dF occurs with fidelity as other natural dNTPs are poorly utilized (*8*). This result as well as other reports using distinct non-natural nucleotides (*1*, *10*, *11*) has led to a model invoking "shape complementarity" as an important determinant for efficient DNA polymerization (*12*). In this model, any base pair that adopts a geometrical arrangement in size and shape mimicking a natural Watson−Crick base pair is viewed as being correct by the polymerase and, as a consequence, allows for phosphoryl transfer to occur. Base pairs not conforming to this optimal shape and/or size hinder phosphoryl transfer and are thus excluded from the polymerase's active site. In general, this model provides a reasonable mechanism explaining how polymerases achieve rapid and accurate DNA synthesis by catalyzing the formation of correct base pairs while preventing misincorporation events without the aid of hydrogen bonds.

†This research was supported by funding from the National Institutes of Health (Grant CA118408) and the Skin Cancer Foundation to A.J.B.

*To whom correspondence should be addressed. Telephone: (216) 368-4723. Fax: (216) 368-3395. E-mail: ajb15@case.edu.

[1]Abbreviations: dNTP, deoxynucleoside triphosphate; dAMP, adenosine-2′-deoxyriboside monophosphate; dCMP, cytosine-2′-deoxyriboside monophosphate; dGMP, guanosine-2′-deoxyriboside monophosphate; dTMP, thymine-2′-deoxyriboside monophosphate; dF, 2,4-difluorotoluene; dFMP, 2,4-difluorotoluene-2′-deoxyriboside monophosphate; 5-NITP, 5-nitroindolyl-2′-deoxyriboside triphosphate; 5-NIMP, 5-nitroindolyl-2′-deoxyriboside monophosphate; 5-NapITP, 5-naphthylindolyl-2′-deoxyriboside triphosphate; 5-PhITP, 5-phenylindolyl-2′-deoxyriboside triphosphate; 5-CE-ITP, 5-cyclohexenylindolyl-2′-deoxyriboside triphosphate; 5-CH-ITP, 5-cyclohexylindolyl-2′-deoxyriboside triphosphate.

Published on Web 02/27/2010

However, several kinetic phenomena that cannot be reconciled by a model invoking the exclusive contributions of steric fit and shape complementarity exist. For example, the shape complementarity model predicts that the kinetics for forming a base pair should be identical regardless of which nucleobase is present in the template or used as the incoming nucleotides. This mechanism is operational during the formation of correct Watson−Crick base pairs as dAMP is incorporated opposite T just as efficiently as dTMP is incorporated opposite A. However, this relationship is not valid for the replication of non-natural nucleotides as many are incorporated "asymmetrically". In these cases, polymerases display an unexplained preference for forming one base pair compared to its complement. For example, the *E. coli* Klenow fragment efficiently incorporates deoxyxanthosine-2′-deoxyriboside monophosphate opposite 5-(2,4-diaminopyrimidine) but does not incorporate 5-(2,4-diaminopyrimidine)-2′-deoxyriboside monophosphate opposite a template xanthine (*13*). Other examples include the low catalytic efficiency for incorporation of dFMP opposite A compared to the reciprocal reaction of incorporating dAMP opposite dF (compare k_{cat}/K_m values of 4×10^5 and 26×10^5 M^{-1} min^{-1}, respectively) (*8*, *9*).

In addition to these kinetic abnormalities, the structures of several DNA polymerases bound to DNA show that the templating nucleobase exists in an extrahelical position that precludes direct interactions with the incoming dNTP during the initial stages of the polymerization cycle (*14*−*16*). This unusual orientation casts doubt on models invoking either hydrogen bonding interactions or shape complementarity as the preeminent molecular force for efficient DNA synthesis. As a consequence, other biophysical factors such as desolvation, induced dipole moments, and/or π-electron configuration of the incoming nucleotide and templating nucleobase must play significant roles during polymerization.

To quantify the contributions of these biophysical features, we investigated the kinetic behavior of a high-fidelity DNA polymerase during the replication of a unique non-natural nucleobase, 5-nitroindole (5-NI). Although 5-NI mimics the shape and size of adenine, it is devoid of classical hydrogen bonding interactions. As a consequence, most natural nucleotides are poorly incorporated opposite 5-NI. However, nucleotides possessing high base stacking potential (low solvation energies coupled with large π-electron surface areas) are incorporated opposite the non-natural nucleobase with significantly higher catalytic efficiencies. These data are used to develop a mechanism defining the roles of entropic (nucleobase hydrophobicity) and enthalpic effects (desolvation) during DNA polymerization. In this mechanism, the overall hydrophobic nature of the incoming nucleobase overcomes the lack of hydrogen bonding groups that are generally required for optimal DNA polymerization. However, the lack of hydrogen bonds between base pairs prevents primer extension by hindering translocation of the polymerase to the next templating position. This final aspect is manifest by the appearance of unusually high pyrophosphorolysis activity by the T4 DNA polymerase that is observed only with the non-natural nucleobase in the template. These results collectively provide additional insight into how DNA polymerization can occur without the use of shape complementarity or hydrogen bonds. However, the results also illustrate how the lack of hydrogen bonding interactions adversely affects primer extension and enhances pyrophosphorolysis to prevent complete replication of a non-natural base pair.

MATERIALS AND METHODS

Materials. The exonuclease-deficient mutant of gp43 (Asp-219 to Ala mutation) was purified and quantified as previously described (*17*). Oligonucleotides, including those containing a tetrahydrofuran moiety mimicking an abasic site, were synthesized by Operon Technologies (Alameda, CA). Single-strand and duplex DNA were purified and quantified as described previously (*18*). [γ-^{32}P]ATP was purchased from Perkin-Elmer Life and Analytical Sciences (Boston, MA). Unlabeled dNTPs (ultrapure) were obtained from Pharmacia. Magnesium acetate and Trizma base were from Sigma. Urea, acrylamide, and bisacrylamide were from National Diagnostics (Rochester, NY). 5-Fluorouridine-2′-deoxyriboside triphosphate (5-F-dUTP), 5-aminoallyluridine-2′-deoxyriboside triphosphate (5-AA-dUTP), 2-thiothymine-2′-deoxyriboside triphosphate (2-thio-dTTP), 4-thiothymine-2′-deoxyriboside triphosphate (4-thio-dTTP), 5-propynyluridine-2′-deoxyriboside triphosphate (5-Pro-dUTP), 5-hydroxyluridine-2′-deoxyriboside triphosphate (5-OH-dUTP), 2-amino-2′-deoxyadenosine 5′-triphosphate (2-APTP), 2′-deoxyinosine 5′-triphosphate (dITP), 6-chloropurine-2′-deoxyadenosine 5′-triphosphate (6-Cl-PTP), 6-chloro-2-amino-2′-deoxyadenosine 5′-triphosphate (6-Cl-2-APTP), 7-deaza-2′-deoxyadenosine 5′-triphosphate (7-deaza-dATP), 7-deaza-2′-deoxyguanosine 5′-triphosphate (7-deaza-dGTP), N^2-methyl-2′-deoxyguanosine 5′-triphosphate (N^2-methyl dGTP), O^6-methyl-2′-deoxyguanosine 5′-triphosphate (O^6-methyl-dGTP), and N^6-methyl-2′-deoxyadenosine 5′-triphosphate (N^6-methyl-dATP) were purchased from TriLink Biotechnologies (San Diego, CA). Indolyl-2′-deoxyriboside triphosphate (IndTP), 5-fluoroindolyl-2′-deoxyriboside triphosphate (5-FITP), 5-aminoindolyl-2′-deoxyriboside triphosphate (5-AITP), 5-nitroindolyl-2′-deoxyriboside triphosphate (5-NITP), 5-cyclohexylindolyl-2′-deoxyriboside triphosphate (5-CH-ITP), 5-cyclohexenylindolyl-2′-deoxyriboside triphosphate (5-CE-ITP), 5-phenylindolyl-2′-deoxyriboside triphosphate (5-PhITP), and 5-naphthylindolyl-2′-deoxyriboside triphosphate (5-NapITP) were synthesized and purified as previously described (*19*−*23*). All other materials were obtained from commercial sources and were of the highest quality available.

Polymerization Assays. The assay buffer used in all kinetic studies consisted of 25 mM Tris-acetate (pH 7.5), 150 mM potassium acetate, and 10 mM 2-mercaptoethanol. All assays were performed at 25 °C. Polymerization reactions were monitored by analysis of the products on 20% sequencing gels as previously described (*24*). Gel images were obtained with a Packard PhosphorImager using OptiQuant supplied by the manufacturer. Product formation was quantified by measuring the ratio of ^{32}P-labeled extended and nonextended primer. The ratios of product formation are corrected for the substrate in the absence of polymerase (zero point). Corrected ratios are then multiplied by the concentration of the primer−template motif used in each assay to yield the total product. All concentrations are listed as final solution concentrations.

Determination of Kinetic Parameters for Nucleotide Incorporation. Kinetic parameters, k_{pol}, K_d, and k_{pol}/K_d, for each modified and non-natural nucleotide were determined by monitoring the rate constants for product formation using a fixed amount of the exonuclease-deficient T4 DNA polymerase (1 μM) and DNA substrate (250 nM) at varying concentrations of nucleoside triphosphate (10−500 μM). Aliquots of the reaction mixtures were quenched in 350 mM EDTA (pH 8) at times ranging from 5 to 300 s. In all cases, samples were diluted 1:1 with sequencing gel loading buffer and products were analyzed for

product formation by denaturing gel electrophoresis. Data obtained for DNA polymerization reactions measured under single-turnover reaction conditions were fit with eq 1:

$$y = A(1 - e^{-kt}) + C \quad (1)$$

where A is the burst amplitude, k is the observed rate constant (k_{obs}) in initial product formation, t is time, and C is a defined constant. Data for the dependence of k_{obs} on dNTP concentration were fit with the Michaelis−Menten equation (eq 2) to provide values corresponding to k_{pol} and K_d.

$$k_{obs} = (k_{pol}[dXTP])/(K_d + [dXTP]) \quad (2)$$

where k_{obs} is the observed rate constant of the reaction, k_{pol} is the maximal polymerization rate constant, K_d is the dissociation constant for dXTP, and [dXTP] is the concentration of the non-natural nucleotide substrate.

Primer Extension Assays. Single-turnover conditions were used to measure the rates of extension beyond base pairs formed between 5-NI in the template strand and various natural and non-natural nucleobases in the primer strand. To enzymatically form the various pairing combinations, 500 nM $13/20_{5\text{-NI}}$-mer was first incubated with 1 μM exonuclease-deficient T4 DNA polymerase and 10 mM $Mg(OAc)_2$ in reaction buffer followed by initiation of the polymerization reaction through the addition of 200 μM dXTP. After four half-lives (time needed to achieve 95% production of 14-mer), 500 μM dGTP, the next correct nucleotide, was added to the reaction mixture to allow for extension beyond the formed mispair. At various time intervals (Δt = 1−10 min), 5 μL aliquots of the reaction were quenched in an equal volume of 350 mM EDTA (pH 8.0). The samples were then diluted 1:1 with sequencing gel loading buffer, and products were analyzed for product formation by denaturing gel electrophoresis as described above.

Pyrophosphorolysis Activity. To enzymatically form the 5-NI·5-NI mispair, 500 nM $13/20_{5\text{-NI}}$-mer was first incubated with 1 μM exonuclease-deficient T4 DNA polymerase and 10 mM $Mg(OAc)_2$ in reaction buffer followed by initiation of the polymerization reaction through the addition of 20 μM 5-NITP. After 3 min, 400 μM PP_i was added to the reaction mixture to initiate pyrophosphorolysis. At various time intervals (Δt = 1−10 min), 5 μL aliquots of the reaction mixture were quenched in an equal volume of 350 mM EDTA (pH 8.0). The samples were then diluted 1:1 with sequencing gel loading buffer, and products were analyzed for product formation by denaturing gel electrophoresis as described above.

The ability of various non-natural nucleotides such as 5-NapITP and 5-PhITP to act as the phosphoryl donor was evaluated using a slight modification to the aforementioned protocol. In these experiments, 20 μM 5-NITP was added to the preincubated polymerase−DNA complex to form the 5-NI·5-NI mispair. In this case, however, a fixed concentration of non-natural nucleotide was added rather than PP_i to initiate the pyrophosphorolysis reaction. In these experiments, the concentration of non-natural nucleotide was maintained at its K_d value for incorporation opposite 5-NI (vida supra). After the addition of the non-natural nucleotide, aliquots were quenched as a function of time (Δt = 1−10 min), and the products were analyzed by denaturing gel electrophoresis as described above.

RESULTS

Replication of a "Universal" Non-Natural Nucleotide Occurs in an Asymmetric Fashion. The ability of the exo-nuclease-deficient T4 DNA polymerase to incorporate 5-nitroindolyl-2′-deoxynucleoside monophosphate (5-NIMP) (Figure 1A) opposite natural templating nucleobases and a nontemplating DNA lesion (abasic site) was assessed as previously described (*25*). The data illustrated in Figure 1B recapitulate previous observations that 5-NIMP is preferentially incorporated opposite the nontemplating abasic site (*26*). These data also show that while 5-NIMP is a purine analogue lacking classical hydrogen bonding groups, it is incorporated opposite each of the four natural templating nucleobases with similar efficiencies (Figure 1B). The promiscuous nature of 5-NITP as the incoming nucleotide is consistent with its designation as a universal nucleotide (*27*, *28*) and is attributed to the enhanced base stacking capabilities of 5-nitroindole as it contains significant π-electron density coupled with low solvation energies (*29*).

The nonselective nature of 5-NITP as the incoming nucleotide led to the hypothesis that 5-NI in the template strand should also be highly nonselective; i.e., all four natural nucleotides should be incorporated with similar efficiencies. Representative data provided in Figure 1D provide evidence to the contrary as dAMP and dTMP are the only nucleotides incorporated opposite 5-NI. In addition, the efficiency of their incorporation is very low compared to that of the reciprocal reaction of incorporating 5-NIMP opposite either nucleobase. For example, the first-order rate constant for dAMP incorporation opposite 5-NI (0.0033 ± 0.0005 s^{-1}) is 1300-fold slower than the k_{pol} of 4.4 ± 0.1 s^{-1} measured for the reciprocal reaction of incorporation of 5-NIMP opposite adenine (*26*). Likewise, the k_{obs} value of 0.0024 ± 0.0004 s^{-1} measured for incorporation of dTMP opposite 5-NI is 380-fold slower than the rate constant of 0.9 ± 0.1 s^{-1} measured for incorporation of 5-NIMP opposite thymine (*26*). It should be noted that the rate constants for forming either non-natural base pair are significantly slower than the maximal rate constants of 50−100 s^{-1} measured for formation of a normal Watson−Crick base pair (Table 1) (*17*, *18*). Regardless, the differences in nucleotide utilization as well as the significantly lower rate constants for formation of a base pair containing a non-natural nucleotide indicate that polymerization catalyzed by the bacteriophage T4 DNA polymerases occurs in an asymmetric manner.

Incorporation of Modified Pyrimidine Analogues opposite 5-Nitroindole. The preferential utilization of dTTP could reflect the influence of steric fit and shape complementarity (*7*, *12*) since the overall shape and size of a thymine·5-nitroindole pair are more like those of a Watson−Crick base pair than those of an adenine/guanine·5-nitroindole base pair (Figure 2A). To evaluate this possibility, various dTTP analogues illustrated in Figure 2B were tested for incorporation opposite 5-NI. As shown in Figure 2C, only 2-thiothymine-2′-deoxyriboside monophosphate (2-thio-dTMP) is incorporated opposite 5-NI to an appreciable extent. The dissociation constant (K_d)[2] and maximal polymerization rate constant (k_{pol}) for incorporation of 2-thio-dTMP opposite 5-NI were measured as previously described (*26*). The data provided in Figure 2D illustrate the dependence of 2-thio-dTTP concentration on the kinetics of polymerization. These time courses are unique as both the amplitudes in product formation and the affiliated rate constants show a dependence on 2-thio-dTTP concentration. Each time course is best defined as a

[2]Since the reactions were performed using single-turnover conditions and the rate-limiting step for incorporation is likely to be the conformational change preceding phosphoryl transfer, the measured K_m values closely approximate a true dissociation constant (K_d).

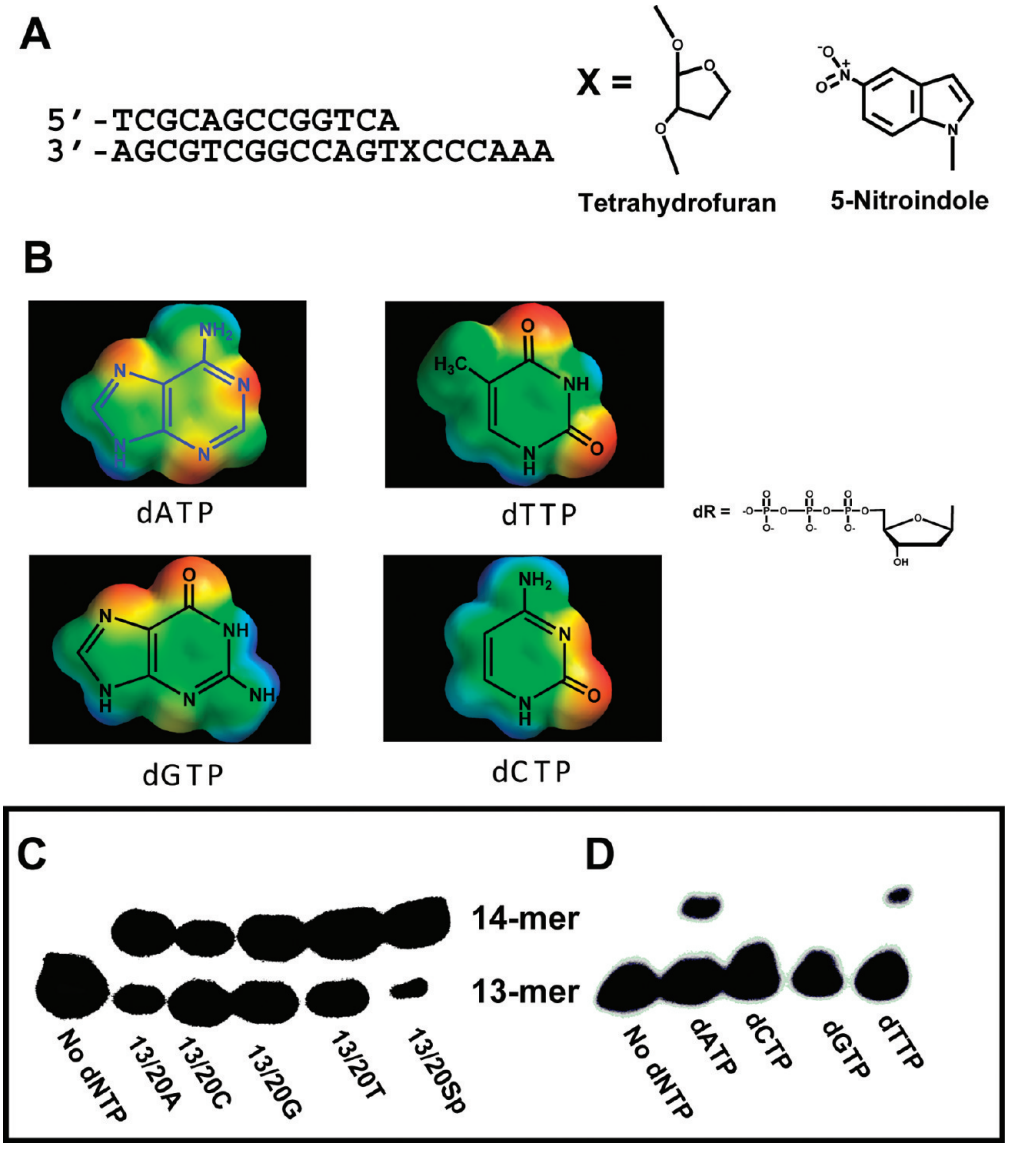

FIGURE 1: (A) Defined DNA substrates used for kinetic analysis. (B) Structures of 2′-deoxynucleoside triphosphates used in this study. For the sake of convenience, dR is used to represent deoxyribose triphosphate. (C) Representative gel electrophoresis for the incorporation of 25 μM 5-NITP opposite all four templating nucleobases (A, C, G, and T) or opposite an abasic site. (D) Representative gel electrophoresis for the incorporation of natural nucleotides (500 μM) opposite 5-nitroindole present in the templating strand.

single exponential from which k_{obs} values were obtained. The plot of k_{obs} versus 2-thio-dTTP concentration is hyperbolic (Figure 2E), and a fit of the data to the Michaelis−Menten equation (*30*) yields a k_{pol} value of 0.047 ± 0.003 s^{-1}, a K_d value of 55 ± 12 μM, and a k_{pol}/K_d value of 855 ± 90 M^{-1} s^{-1}.

The incorporation of 2-thio-dTMP could reflect the contributions of steric fit as the replacement of oxygen with sulfur causes a subtle increase in size of the incoming nucleobase which could allow for more favorable interactions with the templating 5-NI (Figure 1A of the Supporting Information). Indeed, analogous replacement of oxygen with sulfur at the corresponding 4-position of dTMP [4-thiothymine-2′-deoxyriboside monophosphate (4-thio-dTMP)] is expected to clash with the nitro group of 5-NI (Figure 1B of the Supporting Information). In this case, the lack of shape complementarity could explain why 4-thio-dTMP is not incorporated opposite 5-NI (Table 1). This interpretation would be consistent with recent work from the Kool laboratory demonstrating that subangstrom increases in the size of the incoming pyrimidine triphosphate can significantly influence the dynamics of nucleotide incorporation opposite a templating nucleobase (*31*, *32*). However, the inability of the T4 DNA polymerase to incorporate other analogues such as 5-F-dUMP and 5-OH-dUMP that are similar in shape and size to dTMP argues that biophysical features distinct from shape complementarity and steric fit play important roles as well.

Incorporation of Modified Purine Analogues opposite 5-Nitroindole. The incorporation of dTMP and 4-thio-dTMP opposite 5-NI could reflect the influence of optimized base pair geometry. However, this cannot explain the efficient incorporation of dAMP opposite the non-natural nucleobase. To further investigate this phenomenon, several modified dATP and dGTP analogues (Figure 3A) were tested for incorporation opposite 5-NI. Gel electrophoresis data provided in Figure 3B show that analogues such as N^6-methyl-dAMP, 2-APMP, 6-Cl-2-APMP, and O^6-methyl-dGMP are incorporated opposite 5-NI with surprisingly high efficiencies. Of these four modified purines, only N^6-methyl-dATP displays saturation kinetics (data not shown) from which a k_{pol} of 0.017 ± 0.003 s^{-1}, a K_d of 21 ± 7 μM, and a k_{pol}/K_d of 810 ± 100 M^{-1} s^{-1} were obtained (Table 1). The other three analogues (2-APTP, 6-Cl-2APTP, and O^6-methyl-dGTP) do

Table 1: Summary of Kinetic Parameters for the Incorporation of Natural and Modified Nucleotides opposite 5-Nitroindole by the Bacteriophage T4 DNA Polymerase[a]

analogue	K_d (μM)	k_{pol} (s^{-1})	k_{pol}/K_d (M^{-1} s^{-1})	volume (Å^3)[b]	dipole moment (D)[c]	solvation energy (kcal/mol)[d]
dATP → 5-NI	> 500	~0.0033	6	124.5	2.57	−18.906
dATP → T[e]	10 ± 1	100 ± 10	10^7			
dGTP → 5-NI	ND[f]	ND[f]	ND[f]	131.9	6.93	−24.914
dGTP→ C[g]	5 ± 1	50 ± 7	10^7			
dCTP → 5-NI	ND[f]	ND[f]	ND[f]	104.9	6.62	−23.778
dTTP → 5-NI	> 500	~0.0024	5	119.9	4.17	−11.840
5-F-dUTP	ND[f]	ND[f]	ND[f]	106.7	3.97	−11.079
5-AA-dUTP	ND[f]	ND[f]	ND[f]	162.9	3.33	−15.857
4-thio-dTTP	ND[f]	ND[f]	ND[f]	128.8	4.49	−13.650
2-thio-dTTP	55 ± 12	0.047 ± 0.003	855 ± 90	129.2	4.47	−14.378
2-pro-dUTP	ND[f]	ND[f]	ND[f]	148.5	4.38	−13.609
5-OH-dUTP	ND[f]	ND[f]	ND[f]	109.0	5.27	−17.524
N^6-Me-dATP	21 ± 7	0.017 ± 0.003	810 ± 100	145.3	2.52	−15.849
O^6-Me-dGTP	> 500	~0.008	16	152.1	3.03	−19.303
2-APTP	> 500	~0.0033	7	124.8	3.29	−19.487
dITP	ND[f]	ND[f]	ND[f]	121.5	5.16	−22.850
7-deaza-dATP	ND[f]	ND[f]	ND[f]	130.9	3.88	−16.963
7-deaza-dGTP	ND[f]	ND[f]	ND[f]	138.4	4.88	−18.533
6-Cl-dATP	> 500	~0.010	20	125.9	4.86	−16.147
6-Cl-2APTP	ND[f]	ND[f]	ND[f]	136.1	4.85	−18.813

[a]Assays were performed using 1 μM exonuclease-deficient bacteriophage T4 DNA polymerase, 250 nM 13−20$_{5\text{-NI}}$-mer, and variable concentrations of non-natural nucleotide in the presence of 10 mM Mg^{2+}. [b]Volume (used as an indicator of the relative size of the nucleobase) calculated using Spartan '04. [c]Dipole moments calculated using Spartan '04. [d]Solvation energies for each nucleobase calculated using Spartan '04. [e]Values taken from refs *18* and *17*. [f]No incorporation detected up to a concentration of 500 μM. [g]Unpublished results of A. J. Berdis.

not show saturation kinetics up to concentrations of 500 μM (data not shown), and this prohibits the measurement of accurate K_d and k_{pol} values. However, it is possible to use the linear portion of a Michealis−Menten curve to accurately measure the catalytic efficiencies (k_{pol}/K_d) for incorporation opposite 5-NI (Table 1). It is quite intriguing that the overall catalytic efficiency of 810 M^{-1} s^{-1} for N^6-methyl-dATP is essentially identical to that for 2-thio-dTTP (k_{pol}/K_d = 855 M^{-1} s^{-1}) since the nucleotides differ greatly with respect to shape, size, and potential hydrogen bonding interactions. It is even more surprising that the larger purine analogue has an ~2-fold lower K_d value than the smaller pyrimidine (compare K_d values of 21 and 55 μM for N^6-Me-dATP and 2-thio-dTTP, respectively).

Incorporation of Non-Natural Nucleoside Monophosphates as Probes for the Involvement of Base Stacking. The influence of π-electron density and hydrophobicity on nucleotide incorporation was assessed by measuring the ability of the T4 DNA polymerase to incorporate various 5-substituted indolyl nucleotides (Figure 4A) opposite 5-NI. Initial screening revealed that non-natural nucleotides such as 5-PhIMP and 5-CE-IMP are incorporated opposite 5-NI (Figure 4B) much more effectively than the natural nucleotides, dAMP and dTMP, or any of their modified counterparts. In addition, the kinetics of incorporation of 5-PhIMP opposite 5-NI are similar to those previously described for 2-thio-dTMP as both the rate constants and amplitudes for product formation are dependent upon 5-PhITP concentration (Figure 4C). The corresponding plot of k_{obs} versus 5-PhITP concentration (Figure 4D) yields a k_{pol} value of 0.107 ± 0.005 s^{-1}, a K_d value of 8.7 ± 1.1 μM, and a k_{pol}/K_d value of 12300 ± 500 M^{-1} s^{-1}. Similar results were obtained with other non-natural nucleotides such as IndTP, 5-FITP, 5-NITP, and 5-CH-ITP (data not shown), and their kinetic parameters are summarized in Table 2.

The non-natural nucleotide, 5-NapITP, displays unique kinetic behavior as the plot of k_{obs} versus nucleotide concentration provides a pattern consistent with substrate-induced inhibition (Figure 5A). A fit of the data to the equation describing competitive substrate inhibition (*33*) yields a k_{pol} value of 0.029 ± 0.009 s^{-1}, a K_d of 17 ± 8 μM, a k_{pol}/K_d of 1720 M^{-1} s^{-1}, and a K_i of 41 ± 15 μM. Similar data were obtained for the incorporation of 5-CE-IMP (data not shown). In both cases, the appearance of substrate-induced inhibition is dependent upon the nature of the templating nucleobase as this phenomenon is not observed for their incorporation opposite templating nucleobases (*19*) or damaged DNA (*34*).

Unusual Pyrophosphorolysis Activity Accounts for the Appearance of Substrate-Induced Inhibition. Inhibition of polymerase activity by nucleotide substrates has been observed primarily during mismatch DNA synthesis, i.e., the misincorporation of dAMP opposite C (*35*−*37*). Since this phenomenon occurs using high nucleotide concentrations (> 1 mM), it is typically attributed to the nonproductive binding of an incorrect nucleotide to the polymerase−DNA complex or to the binding of nucleotide to free polymerase to form the pol−dNTP complex. In this later case, the formation of the pol−dNTP complex causes inhibition by preventing DNA binding to form the catalytically competent pol−DNA−dNTP ternary complex .

An alternative possibility for explaining substrate inhibition is that the nucleotide can act as a substrate for the pyrophosphorolysis reaction to directly reverse the forward polymerization reaction (Figure 5B). This mechanism was evaluated via measurement of the pyrophosphorolysis activity of the exonuclease-deficient T4 DNA polymerase on the 5-NI·5-NI mispair. Briefly, this mispair was formed in situ via addition of 20 μM 5-NITP to the preincubated polymerase−13/20$_{5\text{-NI}}$-mer complex.

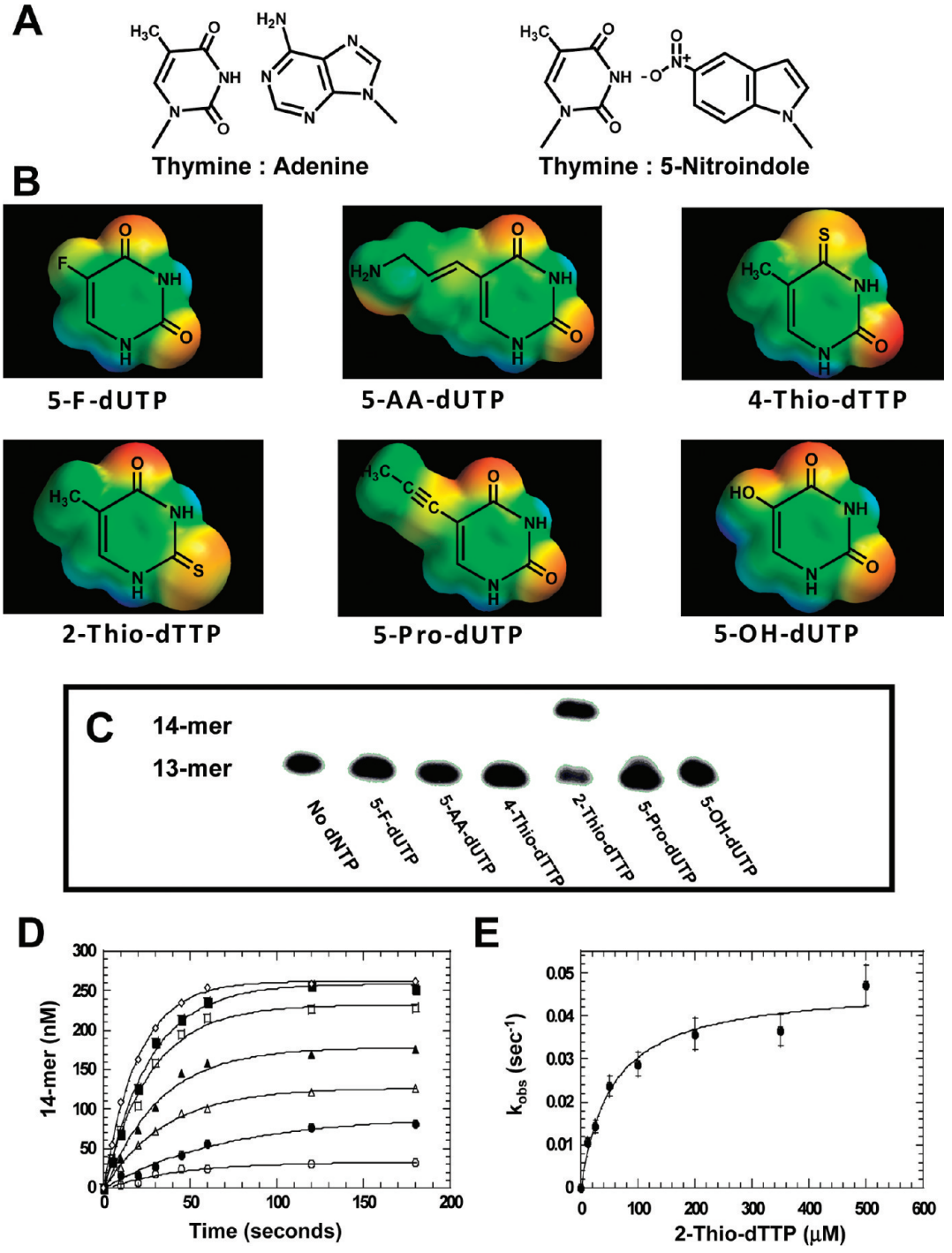

FIGURE 2: (A) Comparison of the structure of a natural thymine·adenine base pair vs a thymine·5-nitroindole base pair. (B) Structures of modified pyrimidine-2′-deoxynucleoside triphosphates used in this study. For the sake of convenience, only the nucleobase portion of the modified pyrimidine is provided to show clarity with respect to surface ionization potential. Surface ionization potentials for each nucleobase were generated using Spartan '04. Red indicates the most electronegative regions, green neutral regions, and blue electropositive regions. The partial atomic charges were calculated using the DFT 6-31G** method and basis set. (C) Representative gel electrophoresis for the incorporation of modified pyrimidine triphosphates (500 μM) opposite 5-nitroindole present in the templating strand. (D) Rate constants for 2-thio-dTTP opposite 5-NI as a function of nucleotide concentration. Assays were performed using 1 μM gp43 exo$^-$, 250 nM 13/20$_{5\text{-NI}}$-mer, 10 mM $Mg(OAc)_2$, and 2-thio-dTTP at variable concentrations: 10 (○), 25 (●), 50 (△), 100 (▲), 200 (□), 350 (■), and 500 μM (◇). The solid lines represent fits of the data to a single exponential. (E) k_{obs} values (●) were plotted vs 2-thio-dTTP concentration and fit using the Michaelis−Menten equation to determine the following values: $K_d = 55 \pm 12$ μM, $k_{pol} = 0.047 \pm 0.003$ s^{-1}, and $k_{pol}/K_d = 855 \pm 90$ M^{-1} s^{-1}.

After 3 min (Δt_1 of more than four half-lives), 400 μM PP_i was added to initiate pyrophosphorolysis, and aliquots of the reaction mixture were quenched into EDTA as a function of time (Δt_2 = 1−10 min). The results provided in Figure 5C show that the addition of 400 μM PP_i leads to a reduction in the amount of enzymatically formed 14-mer, consistent with pyrophosphorolysis-mediated degradation of the primer. Pyrophosphorolysis activity is dependent upon the composition of the templating base since this activity is not observed when 5-NI is paired opposite thymine or an abasic site (Figure 2 of the Supporting Information).

To further investigate this unique pyrophosphorolytic activity, we measured the ability of PP_i to remove other non-natural

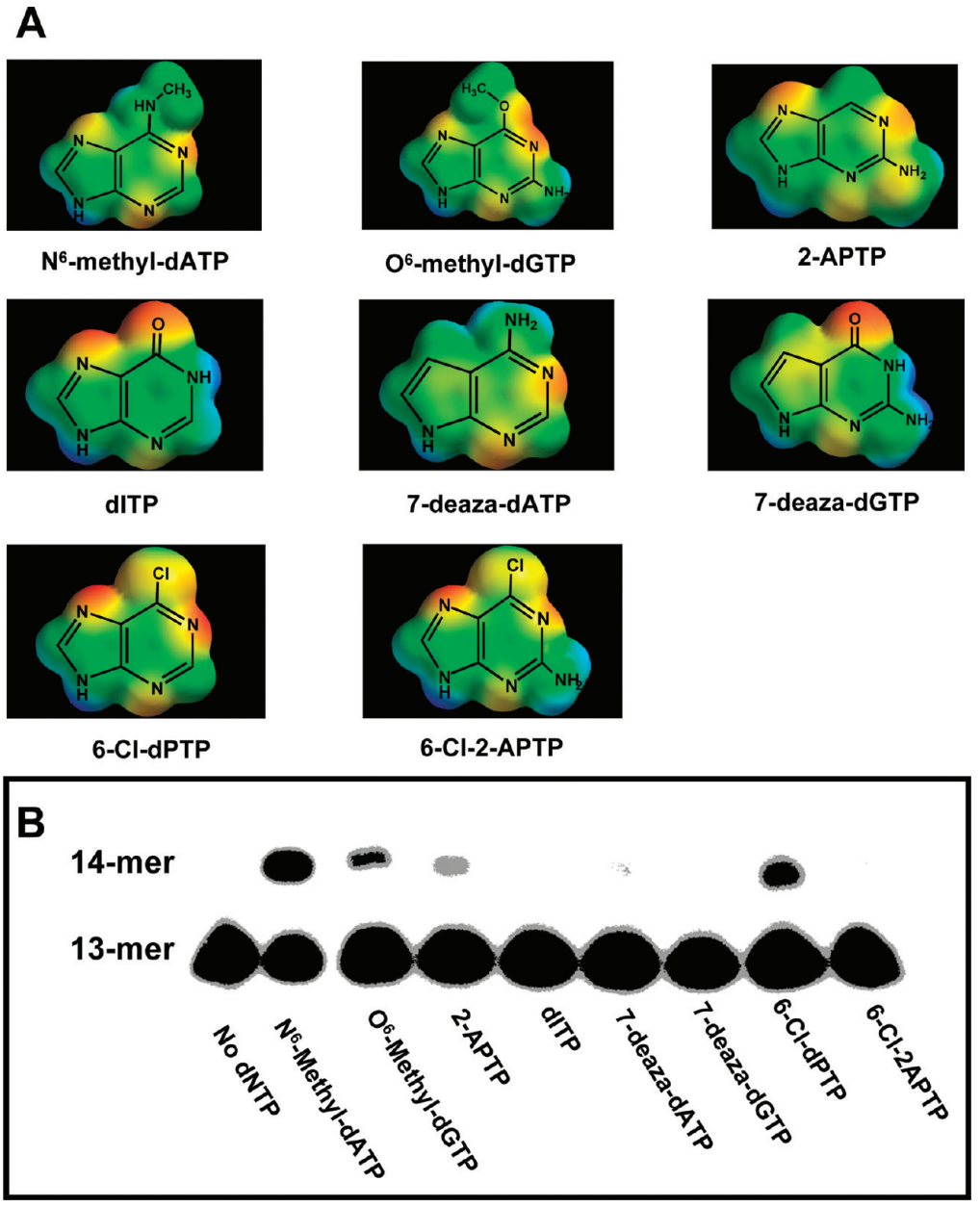

FIGURE 3: (A) Structures of modified purine-2′-deoxynucleoside triphosphates used in this study. For the sake of convenience, only the nucleobase portion of the modified purine is provided for the sake of clarity. Surface ionization potentials for each nucleobase are provided for comparison and were generated using Spartan '04. Red indicates the most electronegative regions, green neutral regions, and blue electropositive regions. The partial atomic charges were calculated using the DFT 6-31G** method and basis set. (B) Representative gel electrophoresis for the incorporation of modified purine triphosphates (500 μM) opposite 5-nitroindole present in the templating strand.

nucleotides when paired opposite 5-NI in the template. Each mispair was formed in situ by adding K_d concentrations of the non-natural nucleotide (5-FITP, 5-CE-ITP, 5-PhITP, 5-NapITP, or 2-thio-dTTP) to the preincubated polymerase−:13/$20_{5\text{-NI}}$-mer complex. After four half-lives, 400 μM PP_i was added to initiate pyrophosphorolysis, and aliquots of the reaction mixture were quenched into EDTA as a function of time (data not shown). In all cases, the addition of PP_i causes a reduction in the amount of enzymatically formed 14-mer, consistent with pyrophosphorolysis-mediated degradation of the primer. However, the amount of degradation is dependent upon the composition of the terminal nucleobase. To quantify these differences, each time course was fit to a single exponential to define the rate constant for pyrophosphorolysis (k_{pyro}). On the basis of the magnitude of these k_{pyro} values, the rank order of reactivity for the terminal base is as follows: 5-FInd > 2-thio-dT > 5-PhInd > 5-NInd ≫ 5-CE-Ind and 5-NapInd. In general, the data reveal an inverse correlation between pyrophosphorolysis activity and the base stacking potential of the terminal base.

A slight modification of this experimental paradigm was employed to test the ability of 5-NapITP to directly act as the phosphoryl donor during pyrophosphorolysis. After enzymatic formation of the 5-NI·5-NI mispair (Δt_1 = 3 min), 30 μM 5-NapITP was added to initiate pyrophosphorolysis. As illustrated in Figure 5D, the addition of 5-NapITP causes a rapid degradation of the primer containing the incorporated 5-NIMP (band denoted as "14-NI"). However, the removal of 5-NIMP regenerates the original 13-mer primer which then allows for the incorporation of 5-NapIMP opposite 5-NI (band denoted as "14-Nap"). The production of the 14-Nap band does not simply

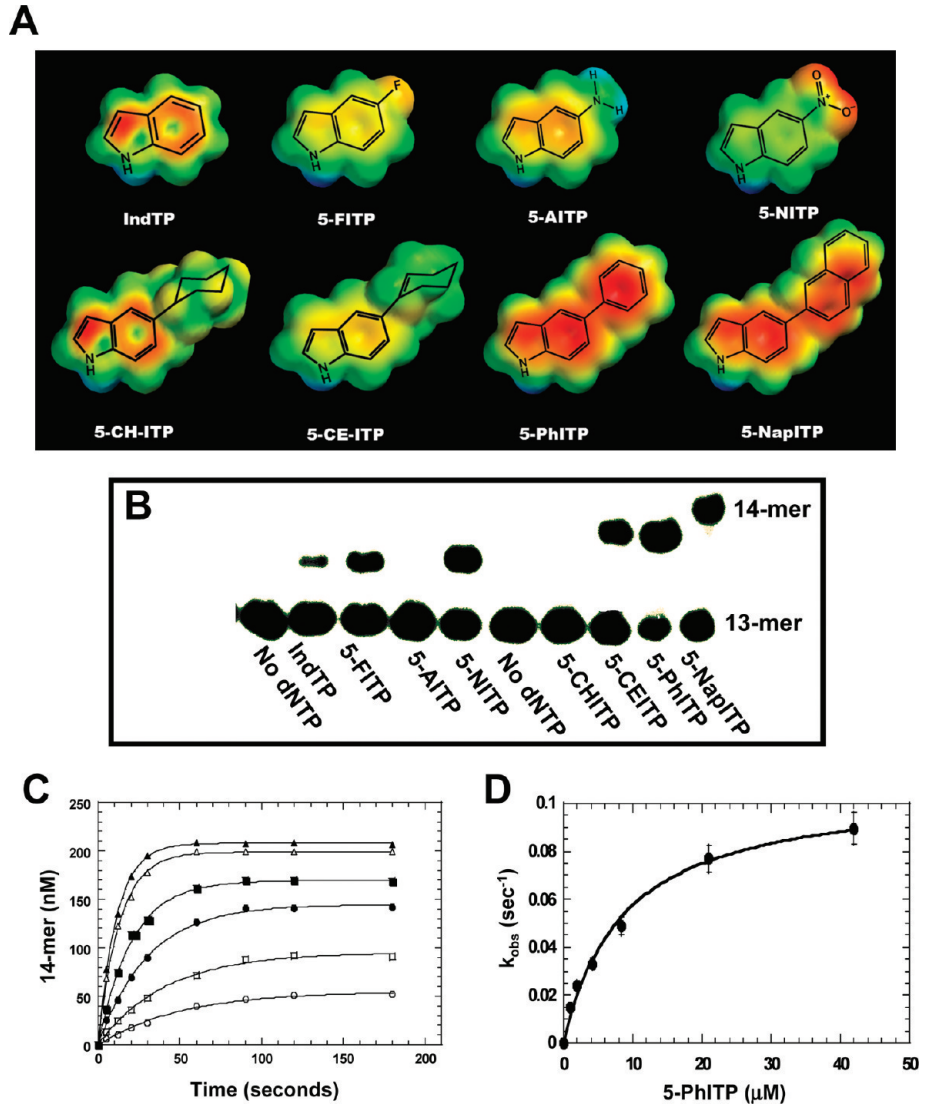

FIGURE 4: (A) Structures of 5-substituted indolyl-2′-deoxynucleoside triphosphates used in this study. Only the non-natural nucleobases are provided for the sake of clarity. Surface ionization potentials for each nucleobase are provided for comparison and were generated using Spartan '04. Red indicates the most electronegative regions, green neutral regions, and blue electropositive regions. The partial atomic charges were calculated using the DFT 6-31G** method and basis set. (B) Representative gel electrophoresis for the incorporation of modified 5-substituted indolyldeoxyribose triphosphates (500 μM) opposite 5-nitroindole present in the templating strand. (C) Rate constants for the incorporation of 5-PhITP opposite 5-NI as a function of 5-PhITP concentration. Assays were performed using 1 μM gp43 exo$^-$, 250 nM 13/20$_{5\text{-NI}}$-mer, 10 mM $Mg(OAc)_2$, and 5-PhITP at variable concentrations: 1 (○), 2 (□), 4 (●), 8 (■), 21 (△), and 42 μM (▲). The solid lines represent fits of the data to a single exponential. (D) k_{obs} values (●) were plotted vs 2-thio-dTTP concentration and fit using the Michaelis−Menten equation to determine the following values: $K_d = 8.7 \pm 1.1$ μM, $k_{pol} = 0.107 \pm 0.005$ s^{-1}, and $k_{pol}/K_d = 12300 \pm 500$ M^{-1} s^{-1}.

Table 2: Summary of Kinetic Parameters for the Incorporation of Non-Natural Nucleotides opposite 5-Nitroindole by the Bacteriophage T4 DNA Polymerase[a]

analogue	K_d (μM)	k_{pol} (s^{-1})	k_{pol}/K_d (M^{-1} s^{-1})	volume (Å^3)[b]	π-electron surface area (Å^3)[c]	dipole moment (D)[d]	solvation energy (kcal/mol)[e]
IndTP	60 ± 10	0.014 ± 0.003	230 ± 20	132.8	148.1	2.11	−5.45
5-FITP	55 ± 10	0.030 ± 0.005	545 ± 35	137.7	148.1	3.57	−4.66
5-AITP	ND[f]	ND[f]	ND[f]	143.2	148.1	1.55	−9.47
5-NITP	32 ± 6	0.027 ± 0.002	840 ± 40	154.5	174.0	7.32	−6.92
5-CH-ITP	13 ± 7	0.006 ± 0.001	460 ± 30	228.9	148.1	1.97	−4.23
5-CE-ITP	63 ± 31	0.10 ± 0.03	1590 ± 250	224.2	181.4	2.06	−5.11
5-PhITP	8.7 ± 1.1	0.107 ± 0.005	12300 ± 500	215.6	225.2	2.66	−6.59
5-NapTP	17 ± 8	0.029 ± 0.009	1720 ± 200	267.5	274.6	2.73	−7.21

[a]Assays were performed using 1 μM exonuclease-deficient bacteriophage T4 DNA polymerase, 250 nM 13−20$_{5\text{-NI}}$-mer, and variable concentrations of non-natural nucleotide in the presence of 10 mM Mg^{2+}. [b]Volume (used as an indicator of the relative size of the nucleobase) calculated using Spartan '04. [c]π-Electron surface area refers to the presence of a conjugated functional group at the 5-position of the indolyl-2-deoxyriboside triphosphate and was calculated using Spartan '04. [d]Dipole moments calculated using Spartan '04. [e]Solvation energies for each nucleobase calculated using Spartan '04. [f]No incorporation detected up to a concentration of 500 μM.

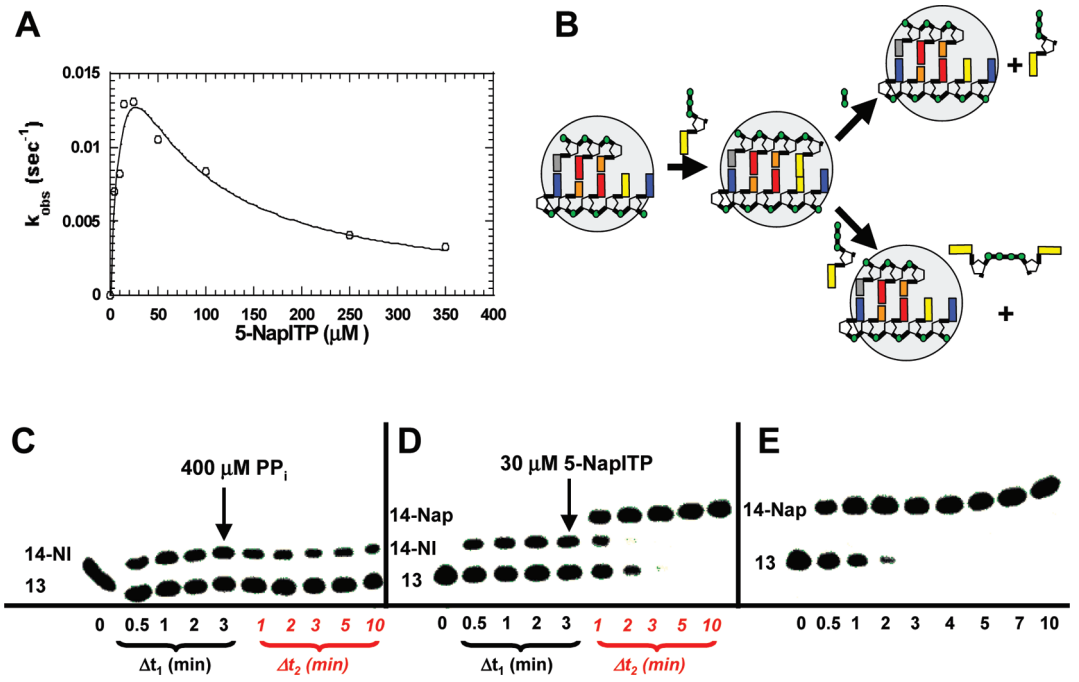

FIGURE 5: (A) Substrate-induced inhibition by 5-NapITP during incorporation opposite 5-nitroindole. The observed rate constants for incorporation (○) were plotted vs 5-NapITP concentration and fit to the equation for competitive substrate inhibition [$k_{obs} = (k_{pol}$-[5-NapITP])/(K_d + [5-NapITP] + K_i[5-NapITP]^2)] to determine the following values: $K_d = 17 \pm 8$ μM, $k_{pol} = 0.029 \pm 0.009$ s^{-1}, $k_{pol}/K_d = 1720 \pm 200$ M^{-1} s^{-1}, and $K_i = 41 \pm 15$ μM. (B) Proposed mechanism for the incorporation and subsequent excision of a non-natural nucleotide via pyrophosphorolysis, the reversal of polymerization. See the text for details. (C) Pyrophosphorolysis of 5-NIMP when paired opposite 5-nitroindole in the template strand. Removal of the enzymatically formed 14-mer is caused by the addition of 400 μM PP_i. See the text for details regarding the experimental design. (D) 5-NapITP-mediated pyrophosphorolysis of 5-NIMP when paired opposite 5-nitroindole in the template strand. Degradation of the enzymatically formed 14-mer caused by the addition of 30 μM 5-NapITP. See the text for further details regarding the dynamics of the pyrophosphorolysis reaction. (E) Incorporation of 30 μM 5-NapITP opposite 5-NI. The identical mobility of the "14-Nap" band compared to the results depicted in panel D indicates that the reaction products do not reflect elongation from 5-NIMP but instead reflect the enzymatic removal of 5-NIMP and subsequent insertion of 5-NapITP opposite 5-NI in the template.

represent elongation of the 14-NI-mer band since control experiments validate that the band denoted as 14-Nap represents incorporation of 5-NapITP opposite 5-NI (Figure 5E).

We also assessed if other non-natural nucleotides could act as phosphoryl transfer donors to remove 5-NIMP as the terminal primer base. Since this assay relies on measuring differences in the mobility of DNA primers via denaturing gel electrophoresis, there are limitations about which non-natural nucleotides could be tested. Specifically, only relatively "large" non-natural nucleotides such as 5-PhITP, 5-CE-ITP, and 5-CH-ITP could be tested as they display significant differences in mobility during electrophoresis. In all cases, the addition of these non-natural nucleotides caused a reduction in the amount of enzymatically formed 14-mer (Figure 3 of the Supporting Information). In these cases, the extent of degradation depends upon the composition of the non-natural nucleotide acting as the phosphoryl transfer donor. As before, these differences were quantified through fits of the data to a single exponential, and the rank order of reactivity for these nucleotides is as follows: 5-NapITP and 5-CE-ITP ≫ 5-PhITP and 5-CH-ITP. These data suggest a correlation between pyrophosphorolysis activity and the base stacking potential of the phosphoryl transfer donor.

Nucleotide Incorporation in the Presence of Exonuclease Activity. Like most high-fidelity DNA polymerases, the bacteriophage T4 enzyme possesses a vigorous exonuclease activity that plays a significant biological role in maintaining genomic fidelity. Although we have demonstrated that pyrophosphorolytic activity participates in the removal of nucleotides paired opposite 5-NI, it is important to examine the capacity of exonuclease excision to effectively remove nucleotides paired opposite a noncanonical nucleobase. This was accomplished by comparing the ability of the wild-type bacteriophage polymerase (gp43exo$^+$) versus the exonuclease-deficient polymerase, gp43 exo$^-$, to stably insert 5-NIMP opposite 5-NI. As illustrated in Figure 6A, gp43exo$^-$ efficiently incorporates 5-NIMP opposite its non-natural counterpart while barely detectable levels of 5-NIMP incorporation are observed using the wild-type polymerase. Similar results were obtained using other non-natural nucleotides such as 5-PhITP and 5-CE-ITP (Figure 4 of the Supporting Information). In general, the reduced amount of product formation using gp43exo$^+$ infers enzymatic removal of the non-natural nucleotide after it is incorporated.

To validate this conclusion, the efficiency of nucleotide removal via exonuclease proofreading by gp43exo$^+$ was directly compared to removal catalyzed by pyrophosphorolysis. This was achieved by first forming the 5-NI·:5-NI mispair in situ by adding 20 μM 5-NITP to the preincubated gp43 exo$^-$−13/20$_{5\text{-NI}}$-mer complex. After 3 min (Δt_1 of more than four half-lives), 400 μM PP_i was added to initiate pyrophosphorolysis, and aliquots of the reaction mixture were quenched into EDTA as a function of time (Δt_2 = 15−180 s). Representative gel electrophoresis data provided in Figure 6B (left panel) recapitulate results of earlier experiments as the addition of PP_i causes a reduction in the amount of 14-mer. To measure exonuclease degradation of the the 5-NI·5-NI mispair, a similar experiment was performed in 2 μM gp43 exo$^+$ instead of 400 μM PP_i. As illustrated in Figure 6B (right), the addition of the wild-type polymerase leads to a rapid degradation of the 14-mer ($k_{obs} > 0.1$ s^{-1}).

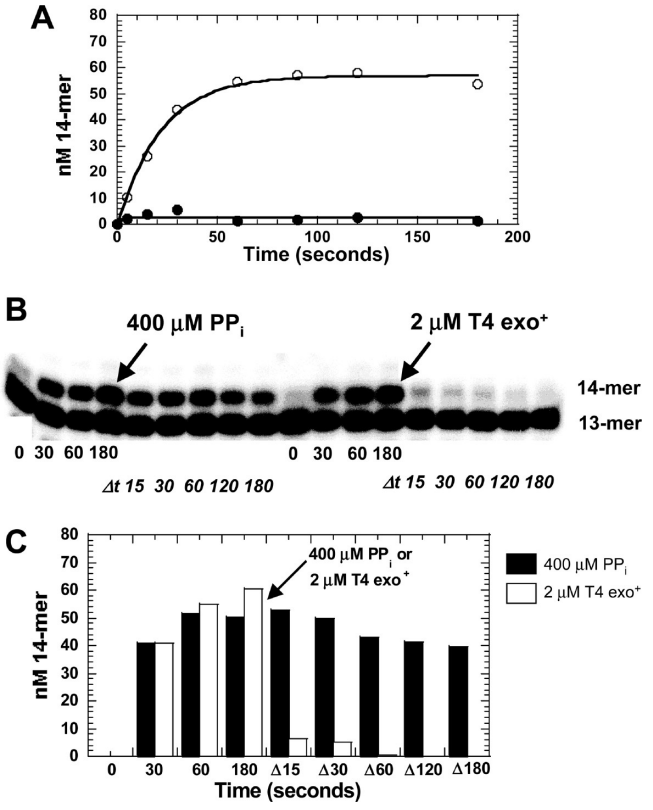

FIGURE 6: (A) Time course for the incorporation of 5-NIMP opposite 5-NI using either gp43 exo$^-$ (○) or gp43 exo$^+$ (●). Assays were performed using 500 nM gp43 exo$^-$ or gp43 exo$^+$, 250 nM 13/20$_{5\text{-NI}}$-mer, 10 mM $Mg(OAc)_2$, and 150 μM 5-NITP. The solid lines represent fits of the data to a single exponential. (B) Gel electrophoresis data comparing pyrophosphorolysis (left) vs exonuclease excision (right) of 5-NIMP paired opposite 5-nitroindole in the template strand. Pyrophosphorolytic removal of the enzymatically formed 14-mer occurs after the addition of 400 μM PP_i. Exonuclease removal of the enzymatically formed 14-mer occurs after the addition of 2 μM gp43 exo$^+$. See the text for details regarding experimental design. (C) Quantification of gel electrophoresis data comparing pyrophosphorolysis vs exonuclease excision of 5-NIMP paired opposite 5-nitroindole.

It is difficult to unambiguously compare the rate constants for nucleotide removal via exonuclease proofreading versus pyrophosphorolysis activity due to differences in reaction conditions.[3] However, quantification of the gel electrophoresis data provided in Figure 6C validates that nucleotide removal occurs far more efficiently via exonuclease excision than by pyrophosphorolysis.

The Absence of Hydrogen Bonds Prevents Primer Extension. Single-turnover conditions were used to measure the rates of extension beyond various natural (dAMP and dTMP), modified (2-thio-dTMP, N^6-methyl-dAMP, O^6-methyl-dGMP, and 2-APMP), and non-natural nucleotides (5-NIMP, 5-PhIMP, and 5-FIMP) paired opposite a template 5-NI. Briefly, mispairs were formed in situ by adding 100 μM nucleotide to the preincubated gp43exo$^-$−13/20$_{5\text{-NI}}$-mer complex. After several minutes to allow for the formation of 14-mer (typically a Δt_1 of 5 min), 500 μM dGTP was added to initiate extension beyond the mispair and aliquots of the reaction mixture were quenched into EDTA as a function of time (Δt_2 = 1−10 min). Under these conditions, extension beyond any base pair combination containing 5-NI in the template was not observed, even in the absence of exonuclease proofreading activity (data not shown).

DISCUSSION

DNA polymerases are remarkably efficient enzymes as they can copy thousands of base pairs per second with an incredible degree of accuracy [~1 mistake every 10^6 opportunities (*38*, *39*)]. They are also enigmatic as they are sufficiently versatile to recognize four distinct pairing partners while capable of maintaining selectivity by inserting only one of four potential dNTPs opposite a template base. Several models have been proposed to account for this dynamic behavior and range from the exclusive utilization of hydrogen bonding interactions to base pair recognition using shape and size complementarity. In this work, we used the unique biophysical properties of 5-NI to further evaluate the contribution of shape, size, and other biophysical features such as nucleobase hydrophobicity and π-electron surface area during polymerization. The significant findings of this report include (a) evidence for asymmetry during the replication of a non-natural nucleobase by the high-fidelity bacteriophage T4 DNA polymerase, (b) the facile incorporation of hydrophobic nucleotides opposite 5-NI which provides evidence of a model invoking desolvation as the predominant molecular force during polymerization, (c) extension of this model to describe the importance of desolvation during the formation of natural Watson−Crick base pairs, and (d) evidence of an enhancement in pyrophosphorolysis activity during the replication of non-natural nucleobases. Each of these points is discussed in more detail below to emphasize their mechanistic ramifications.

Polymerization Occurs in the Absence of Hydrogen Bonds and Shape Complementarity. 5-NI is a non-natural nucleobase that mimics the shape and size of adenine yet is devoid of classical hydrogen bonding functional groups. Although 5-NI is a purine analogue, the non-natural nucleobase is not replicated like a normal templating nucleobase. Instead, the replication of 5-NI is surprisingly similar to the replication of the nontemplating abasic site. This is based upon several key pieces of kinetic data. First, of the four natural nucleotides, dAMP is preferentially incorporated opposite both 5-NI and an abasic site (*26*). Second, modified purines such as N^6-Me-dAMP and O^6-Me-dGMP that possess enhanced base stacking capabilities are incorporated opposite 5-NI and the abasic site much more efficiently than their unmodified natural counterparts (*29*). Finally, the most effective substrates in both cases are 5-substituted indolyl nucleotides that are hydrophobic and contain significant π-electron density (*19*, *22*). However, it is noteworthy that the catalytic efficiencies for their incorporation opposite 5-NI are ~100-fold lower compared to the efficiency of incorporation opposite an abasic site (*19*, *22*). It is interesting that this difference is not caused by perturbations in binding affinities since the K_d values for these analogues are essentially identical regardless of templating base composition. For example, the K_d of 32 μM for 5-NITP with 5-NI containing DNA is identical to the value of 36 μM measured with thymine and only ~2-fold higher than the K_d of 18 μM using abasic site-containing DNA (*26*). Instead, the low catalytic efficiency is caused by large reductions in the k_{pol} values.

This final aspect is noteworthy since the k_{pol} values for these non-natural nucleotides opposite an abasic site are highly sensitive to the overall π-electron surface area of the incoming

[3]Exonuclease proofreading is a first-order reaction; pyrophosphorolysis is a second-order reaction. As such, it is difficult to make accurate mechanistic deductions based upon a simple comparison of kinetic rates for the two reactions.

nucleotide (*23*). This relationship does not exist for their incorporation opposite 5-NI since 5-CH-IMP and 5-FIMP, which lack extensive π-electron density, are incorporated as efficiently as analogues such as 5-PhIMP and 5-NIMP that contain significantly larger π-electron surface areas. The common feature among these four non-natural nucleotides is their hydrophobic nature, and this provides a molecular basis for their insertion opposite an equally hydrophobic nucleobase (vida supra). Indeed, hydrophobic effects likely explain why dAMP and dTMP are the only two natural nucleotides incorporated opposite 5-NI as they possess the lowest solvation energies among the four natural nucleobases (*40*, *41*). Consistent with this mechanism is the fact that 5-AITP, the only hydrophilic non-natural nucleotide tested, is not incorporated opposite 5-nitroindole.

How Much Does Desolvation Contribute toward DNA Polymerization? The importance of hydrophobicity and desolvation is evident via examination of the structure of duplex DNA. The interior of the helix is devoid of water and thus classified as a hydrophobic environment that is essential for the formation of the network of correct hydrogen bonds between base pairs. Creating this hydrophobic environment during DNA polymerization is challenging since water molecules surrounding the functional groups of the incoming dNTP must be removed prior to the formation of hydrogen bonds within the interior of the DNA helix. However, the replication of hydrophobic, non-natural nucleobases such as 5-nitroindole circumvents the requirement for a desolvation step, and thus, only nucleotides that are also relatively hydrophobic are effectively incorporated.

This conclusion is consistent with results reported by the Romesberg group who developed a series of novel base pair combinations using hydrophobic packing interactions rather than hydrogen bonds or shape complementarity (*42*, *43*). This group proposed that interactions between two hydrophobic nucleobases should be stronger than those made between a mixed base pair composed of a hydrophobic base paired opposite a hydrophilic one. Indeed, the catalytic efficiencies for incorporating a natural dNMP opposite a hydrophobic base such as 7-azaindole is ~100-fold lower than for incorporating the hydrophobic isocarbostyril nucleotide opposite 7-azaindole (*44*). Furthermore, this model provides a comprehensive mechanism for the maintenance of replication fidelity as the misinsertion of any natural dNMP opposite a hydrophobic nucleobase is hindered due to unfavorable enthalpic interactions. However, this improvement in fidelity does not extend to the enzymatic formation of a completely hydrophobic base pair. In fact, fidelity cannot be achieved during the replication of two distinct hydrophobic bases due to the ease of enzymatically forming self-pairs. One relevant example of this phenomenon is the higher catalytic efficiency for incorporating dFMP opposite a template dF compared to the incorporation of dAMP, the "preferred" shape partner for dF (*45*). In general, reductions in solvation energies lower entropic penalties and favor nucleotide incorporation. However, they also produce negative effects on selectivity as a hydrophobic base can be efficiently incorporated opposite any other hydrophobic base regardless of shape and/or size.

It is also important to compare the kinetic behavior for forming a mixed (natural·non-natural) base pair such as dAMP·5-NI and dTMP·5-NI with that of corresponding natural mispairs such as dAMP·dG and dTMP·dG as this provides insight into mechanisms used to achieve polymerization fidelity. A summary of kinetic parameters for these various natural and mixed mismatches is provided in Table 3. In general, the efficiency of forming a mixed mispair such as dAMP·5-NI is identical to that for forming natural mismatches such as dAMP·dG and dAMP·dC. In all three cases, the apparent K_m for the incorrect nucleotide is greater than 500 μM while the rate constant for nucleotide incorporation is exceedingly slow ($< 0.005\ s^{-1}$). Similar results are observed for the misincorporation of dTMP opposite the non-natural nucleobase, 5-NI, and natural nucleobases such as dG or dT. As such, the enzymatic formation of a mixed mispair is kinetically disfavored through similar perturbations in K_m and k_{cat} values as observed during the enzymatic formation of natural purine·purine or purine·pyrimidine mispairs.

Table 3: Comparison of the Kinetic Parameters for the Incorporation of Natural Nucleotides opposite Natural Templating Nucleobases and the Non-Natural Nucleobase, 5-Nitroindole, by the Bacteriophage T4 DNA Polymerase

base pair	K_m (μM)	k_{cat} (s^{-1})	k_{cat}/K_m ($M^{-1}\ s^{-1}$)
dATP·dT[a]	10 ± 1	4 ± 1	400000
dATP·dC[b]	1100 ± 160	0.005 ± 0.001	8
dATP·dA[b]	230 ± 60	0.028 ± 0.002	120
dATP·dG[b]	1280 ± 500	0.0049 ± 0.001	4
dATP·5-NI[c]	> 500	~0.0033	6
dTTP·dA[a]	10 ± 1	4 ± 1	400000
dTTP·dC[b]	not determined	not determined	not determined
dTTP·dG[d]	530 ± 65	0.019 ± 0.002	36
dTTP·dT[b]	1350 ± 400	0.021 ± 0.003	16
dTTP·5-NI[c]	> 500	~0.0024	5

[a]Values taken from ref *17*. [b]Values taken from ref *58*. [c]From this study. [d]Unpublished results of A. J. Berdis.

While natural nucleotides are poorly incorporated opposite a noncanonical nucleobase such as 5-nitroindole, it is clear that increasing the base stacking potential of the incoming nucleotide (either through changes in solvation energies or through increased π-electron surface areas) facilitates enzymatic incorporation. This is consistent with previous reports demonstrating that the high-fidelity bacteriophage T4 DNA polymerase incorporates modified natural nucleotides opposite an abasic site much more efficiently than their unmodified counterparts (*29*). The increase in the level of misincorporation of these nucleotides opposite this nontemplating lesion correlated with their enhanced base stacking properties. However, a similar effect was not observed during their misincorporation opposite templating DNA. This suggests that different biophysical features are employed during the replication of damaged versus nondamaged DNA. Thus, most DNA polymerases behave differently when replicating normal versus damaged nucleic acid. Indeed, high-fidelity polymerases typically misinsert a wrong nucleotide upon encountering damaged DNA, while specialized or "error-prone" DNA polymerases such as pol η and pol ι maintain genomic fidelity by incorporating the "correct" nucleotide opposite the DNA lesion (reviewed in ref *46*).

When Does Desolvation Occur during DNA Polymerization? While these data highlight the importance of desolvation, the more daunting challenge is to define how and when desolvation occurs along the multistep DNA polymerization pathway. For example, desolvation could occur during the binding of the incoming nucleotide, during the conformational change step that precedes phosphoryl transfer, or both (Figure 7).[4] We argue that

[4]We argue that desolvation occurs prior to phosphoryl transfer since water must be removed from the polymerase's active site to avoid hydrolysis reactions that would compete with phosphoryl transfer.

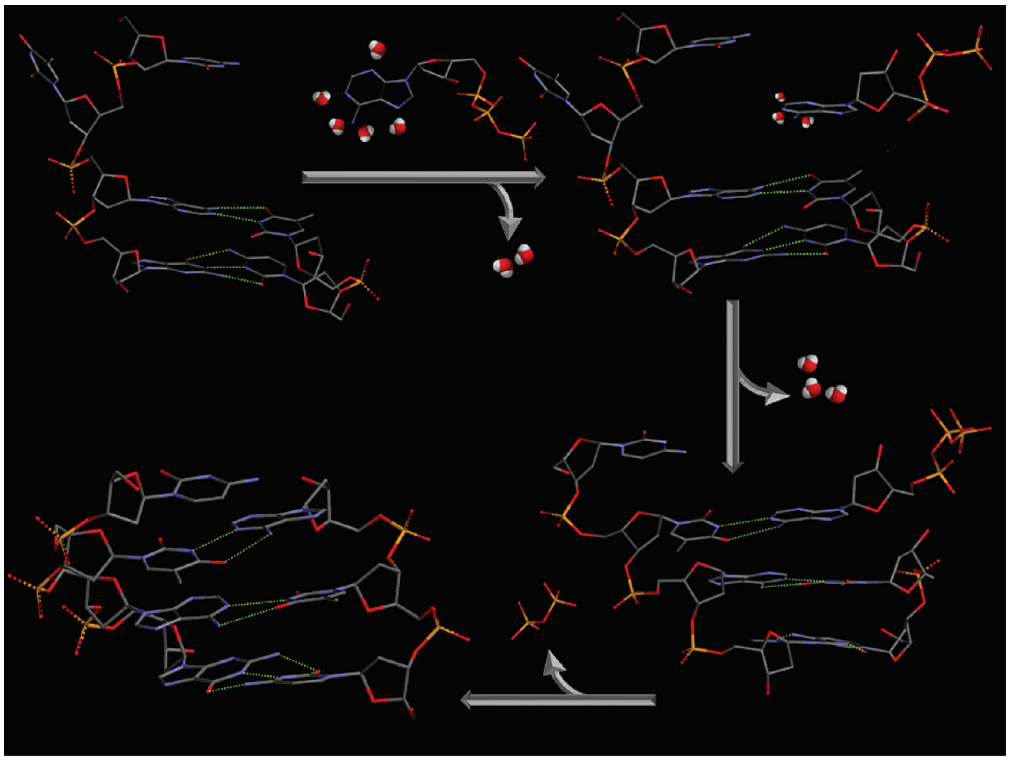

FIGURE 7: Proposed mechanism for desolvation of an incoming nucleotide during DNA polymerization. In this mechanism, the entropic penalty associated with removing water molecules associated with various functional groups is offset by favorable enthalpic contributions caused by the formation of proper hydrogen bond interactions between the two nucleobases. This model for the bacteriophage T4 DNA polymerase invokes an asymmetrical mechanism in which the templating nucleobase is initially in an extrahelical position. Thus, binding of the incoming nucleotide occurs without an obligatory desolvation step. Instead, desolvation of the incoming nucleobase occurs during the conformational change step in which the templating nucleobase and the incoming nucleotide are positioned in an interhelical position to form proper base stacking and hydrogen bonding interactions.

with the bacteriophage T4 DNA polymerase, desolvation likely occurs during the nucleotide binding step since the K_d values for hydrophobic 5-substituted indolyl nucleotides such as 5-PhITP and 5-NapITP are essentially independent of templating nucleobase composition (*21*). In addition, the vast majority of these analogues bind with relatively high affinity (~20 μM) despite the fact that they are not complementary to the shape and/or size of the pairing partner, nor do they contain functional groups that could support enthalpic stabilization via hydrogen bonding interactions. In essence, non-natural nucleotides that can be desolvated easily are thermodynamically more stable in the interior of DNA, and this feature coincides with their low K_d values and more facile incorporation opposite other hydrophobic nucleobases.

Desolvation can also occur during the conformational change step that precedes phosphoryl transfer. This conformational change step was initially attributed to the alignment of the incoming nucleotide with the templating base (*47*). However, this step could also function to exclude water from the polymerase's active site after the binding of the incoming nucleotide. As illustrated in Figure 7, enthalpic penalties associated with removal of water molecules from these various functional groups should be adequately offset by the formation of favorable enthalpic contributions that result from proper hydrogen bonds made between two natural nucleobases. During the enzymatic formation of a mixed hydrophobic−hydrophilic base pair, however, the rate of the conformational change is reduced since the lack of a hydrogen bonding groups precludes the contributions of compensatory enthalpic stabilization inside the DNA helix. Thus, polymerization can occur in the absence of hydrogen bonding potential. However, the efficiency of the process is dramatically reduced.

While our discussion has focused on hydrogen bonding and steric fit recognition, an alternative model invoking positive versus negative selection must also be considered. This model is derived from results generated by the Kuchta laboratory using a series of non-natural nucleotides to probe the determinants used by various DNA polymerases to optimize replication fidelity (*48*, *49*). Results from their studies suggest the use of two orthogonal screens: positive selection for incorporating the correct dNTP and negative selection against incorporating an incorrect dNTP (*48*, *49*). In work relevant to our studies here, the Kuchta laboratory demonstrated that the eukaryotic polymerase, pol α, incorporates 5-nitrobenzimidazole opposite all natural nucleobases at rates comparable to those of normal, correct base pairs (*49*). These results were attributed to a positive versus negative selection mechanism in which the absence or presence of chemical entities that differ from normal purine and pyrimidine bases (i.e., N-3 of purine) defines the ability of a DNA polymerase to recognize the incoming nucleotide as either "right" or "wrong". In other words, the lack of discrimination by pol α against incorporating 5-nitrobenzimidazole results from its inability to recognize 5-nitrobenzimidazole as being wrong since the non-natural nucleotide is so dissimilar from a purine.

At face value, the data obtained here using the bacteriophage T4 DNA polymerase with certain hydrophobic analogues such as 5-NITP, 5-CE-ITP, and 5-NapITP are consistent with this model. These analogues are more efficiently incorporated opposite the hydrophobic 5-nitroindole compared to a hydrophilic nucleobase such as guanine and thus could reflect a negative selection mechanism. As before, the incorporation of these hydrophobic indolyl purine nucleotides results from the absence

of essential features associated with purine nucleotides that are critical for effective discrimination. However, it is impossible to exclude positive selection as the beneficial influence of hydrophobic packing forces may be sufficient for these non-natural nucleotides to be incorporated into duplex DNA (*43*).

The Lack of Primer Extension Enhances Pyrophosphorolysis. In addition to the poor kinetics of nucleotide incorporation opposite 5-NI, the exonuclease-deficient T4 DNA polymerase is unable to extend beyond any base pair containing the non-natural nucleobase in the template. The lack of extension could reflect the absence of hydrogen bonding groups that are essential for polymerase translocation that occurs after nucleotide incorporation (*50*, *51*). Alternatively, this could be caused by the incorrect shape of the formed mispair. Indeed, Romesberg and colleagues showed that the *E. coli* Klenow fragment is unable to extend large, aromatic non-natural nucleobases that result from the formation of an intercalated structure that causes mispositioning of the 3′-OH group in the polymerase's active site to hinder phosphoryl transfer (*43*).

Regardless of the exact molecular mechanism, the increase in the pyrophosphorolysis activity of the bacteriophage T4 DNA polymerase is also consistent with a model invoking inhibition of polymerase translocation. The inability of the polymerase to translocate along DNA containing the non-natural nucleobase would lock the enzyme in a postcatalytic conformation ($E' \cdot DNA_{n+1}$) that is poised to bind pyrophosphate (PP_i) or other phosphoryl donors rather than the next correct nucleotide. The binding of pyrophosphate to form the $E-DNA_{n+1}-PP_i$ complex allows pyrophosphorolysis to occur and generates the $E-DNA_n$ complex and dNTP. This mechanism also explains the appearance of substrate-induced inhibition by non-natural nucleotides, including 5-NapITP and 5-CE-ITP. At low nucleotide concentrations, the production of 14-mer is favored since polymerization activity is higher than pyrophosphorolysis activity. However, as the concentration of the non-natural nucleotide increases, pyrophosphorolysis activity becomes more prevalent such that the 14-mer initially generated via polymerization is removed via pyrophosphorolysis. Precedence for this mechanism comes from studies in which the mechanism of pyrophosphorolysis with HIV reverse transcriptase (RT) was examined because of its importance in the development of drug resistance to chain terminators such as AZT and ddC (*52*, *53*). Although PP_i acts as the normal substrate during pyrophosphorolysis, Meyer et al. demonstrated that ATP can substitute as a phosphoryl donor during this reaction (*54*). Our data using non-natural nucleotides are consistent with this mechanism as increasing the base stacking potential of non-natural nucleotides causes an enhancement in the binding affinity of the $pol-DNA_{n+1}$ complex to facilitate pyrophosphorolysis. In this case, higher pyrophosphorolysis activity is observed with nucleotides such as 5-NapITP and 5-CE-ITP that have greater base stacking potential than analogues such as 5-CH-ITP. A similar correlation is observed between the base stacking potential of the non-natural nucleotide present as the second substrate on the terminal primer. In this case, analogues such as 5-FIMP and 2-thio-dTMP that have low base stacking potential are removed via pyrophosphorolysis significantly faster than analogues such as 5CE-IMP and 5-NapIMP that possess higher base stacking potential.

The enhancement in pyrophosphorolysis also provides a mechanism for explaining the unusual kinetic behavior observed for the incorporation of 2-thio-dTMP, 5-PhIMP, and other non-natural nucleotides opposite 5-NI. As previously described, the time courses of primer elongation with these analogues exhibited unusual effects on both the amplitudes in product formation and the corresponding rate constants for incorporation (vide infra). Similar results were reported by Johnson et al. measuring the enzymatic insertion of AZT-MP opposite adenine by pol γ, the human mitochondrial DNA polymerase (*55*). In this case, the dependence of nucleotide concentration on the amplitude of product formation was argued to be a consequence of a readily reversible polymerization reaction. The data presented here with the bacteriophage T4 polymerase support this model as the polymerization reaction can be easily reversed via pyrophosphorolysis when various nucleotides are incorporated opposite a non-natural nucleobase. Collectively, the enhanced pyrophosphorolysis activity displayed by the T4 DNA polymerase indicates that the phosphoryl transfer step is readily reversible if hydrogen bonding contacts between the formed base pair are not present or if the base pairs are not optimally arranged in the polymerase's active site. Collectively, the lack of translocation and an enhancement of pyrophosphorolysis activity represent significant complications in the application of non-natural nucleotides as chemical tools to expand the genetic code (*56*, *57*).

Is Pyrophosphorolysis Activity Comparable to Exonuclease Proofreading Activity? The enhanced pyrophosphorolysis activity at a noncanonical base can explain the appearance of nucleotide-induced inhibition that is typically observed when misincorporation kinetics catalyzed by exonuclease-deficient DNA polymerases are monitored. In addition, the enhanced pyrophosphorolysis activity also provides a mechanism for explaining why non-natural nucleotides are refractory to elongation, even in the absence of exonuclease proofreading. However, the data provided in Figure 6 clearly show that exonuclease proofreading is far more efficient than pyrophosphorolysis in removing a nucleotide paired opposite a non-natural nucleobase. These kinetic data argue that exonuclease proofreading is more biologically important than pyrophosphorolysis in maintaining genomic fidelity with high-fidelity DNA polymerases. However, this may not be true with "specialized" DNA polymerases that are devoid of exonuclease proofreading activity.

SUPPORTING INFORMATION AVAILABLE

Figure 1A shows the structure of 2-thio-dTMP paired opposite 5-NI, while Figure 1B shows the structure of 4-thio-dTMP paired opposite 5-NI. Figure 2 provides data indicating that pyrophosphorolysis does not occur when 5-NI is paired opposite thymine or an abasic site. Figure 3 provides time courses for pyrophosphorolysis using 5-PhITP, 5-CE-ITP, and 5-CH-ITP as the phosphoryl transfer donor. Figure 4 provides time courses for incorporation of 5-PhIMP (A) and 5-CE-IMP (B) opposite 5-NI using exonuclease-deficient and exonuclease-proficient bacteriophage T4 DNA polymerase. This material is available free of charge via the Internet at http://pubs.acs.org.

REFERENCES

1. Morales, J. C., and Kool, E. T. (1998) Efficient replication between non-hydrogen-bonded nucleoside shape analogs. *Nat. Struct. Biol. 5*, 950–954.
2. Goodman, M. F. (1997) Hydrogen bonding revisited: Geometric selection as a principal determinant of DNA replication fidelity. *Proc. Natl. Acad. Sci. U.S.A. 94*, 10493–10495.
3. Watanabe, S. M., and Goodman, M. F. (1982) Kinetic measurement of 2-aminopurine X cytosine and 2-aminopurine X thymine base pairs

as a test of DNA polymerase fidelity mechanisms. *Proc. Natl. Acad. Sci. U.S.A. 79*, 6429–6433.
4. Topal, M. D., DiGuiseppi, S. R., and Sinha, N. K. (1980) Molecular basis for substitution mutations. Effect of primer terminal and template residues on nucleotide selection by phage T4 DNA polymerase in vitro. *J. Biol. Chem. 255*, 11717–11724.
5. Boosalis, M. S., Mosbaugh, D. W., Hamatake, R., Sugino, A., Kunkel, T. A., and Goodman, M. F. (1989) Kinetic analysis of base substitution mutagenesis by transient misalignment of DNA and by miscoding. *J. Biol. Chem. 264*, 11360–11366.
6. Bebenek, K., Joyce, C. M., Fitzgerald, M. P., and Kunkel, T. A. (1990) The fidelity of DNA synthesis catalyzed by derivatives of *Escherichia coli* DNA polymerase I. *J. Biol. Chem. 265*, 13878–13887.
7. Kool, E. T. (2001) Hydrogen bonding, base stacking, and steric effects in DNA replication. *Annu. Rev. Biophys. Biomol. Struct. 30*, 1–22.
8. Moran, S., Ren, R. X., and Kool, E. T. (1997) A thymidine triphosphate shape analog lacking Watson-Crick pairing ability is replicated with high sequence selectivity. *Proc. Natl. Acad. Sci. U.S.A. 94*, 10506–10511.
9. Moran, S., Ren, R. X., Sheils, C. J., Rumney, S. T., and Kool, E. T. (1996) Non-hydrogen bonding 'terminator' nucleosides increase the 3′-end homogeneity of enzymatic RNA and DNA synthesis. *Nucleic Acids Res. 24*, 2044–2052.
10. Fujiwara, T., Sugiyama, H., Hirao, I., and Yokoyama, S. (2000) Synthesis of 6-(2-thienyl)purine nucleoside derivatives toward the expansion of the genetic code. *Nucleic Acids Symp. Ser.,* 43–44.
11. Hirao, I., Fujiwara, T., Kimoto, M., Mitsui, T., Okuni, T., Ohtsuki, T., and Yokoyama, S. (2000) Unnatural base pairs between 2-amino-6-(2-thienyl)purine and the complementary bases. *Nucleic Acids Symp. Ser.,* 261–262.
12. Kool, E. T. (2002) Active site tightness and substrate fit in DNA replication. *Annu. Rev. Biochem. 71*, 191–219.
13. Lutz, M. J., Held, H. A., Hottiger, M., Hubscher, U., and Benner, S. A. (1996) Differential discrimination of DNA polymerase for variants of the non-standard nucleobase pair between xanthosine and 2,4-diaminopyrimidine, two components of an expanded genetic alphabet. *Nucleic Acids Res. 24*, 1308–1313.
14. Hogg, M., Wallace, S. S., and Doublie, S. (2004) Crystallographic snapshots of a replicative DNA polymerase encountering an abasic site. *EMBO J. 23*, 1483–1493.
15. Hsu, G. W., Ober, M., Carell, T., and Beese, L. S. (2004) Error-prone replication of oxidatively damaged DNA by a high-fidelity DNA polymerase. *Nature 431*, 217–221.
16. Li, Y., Korolev, S., and Waksman, G. (1998) Crystal structures of open and closed forms of binary and ternary complexes of the large fragment of *Thermus aquaticus* DNA polymerase I: Structural basis for nucleotide incorporation. *EMBO J. 17*, 7514–7525.
17. Frey, M. W., Nossal, N. G., Capson, T. L., and Benkovic, S. J. (1993) Construction and characterization of a bacteriophage T4 DNA polymerase deficient in 3′ → 5′ exonuclease activity. *Proc. Natl. Acad. Sci. U.S.A. 90*, 2579–2583.
18. Capson, T. L., Peliska, J. A., Kaboord, B. F., Frey, M. W., Lively, C., Dahlberg, M., and Benkovic, S. J. (1992) Kinetic characterization of the polymerase and exonuclease activities of the gene 43 protein of bacteriophage T4. *Biochemistry 31*, 10984–10994.
19. Zhang, X., Lee, I., Zhou, X., and Berdis, A. J. (2006) Hydrophobicity, shape, and π-electron contributions during translesion DNA synthesis. *J. Am. Chem. Soc. 128*, 143–149.
20. Zhang, X., Lee, I., and Berdis, A. J. (2004) Evaluating the contributions of desolvation and base-stacking during translesion DNA synthesis. *Org. Biomol. Chem. 2*, 1703–1711.
21. Zhang, X., Lee, I., and Berdis, A. J. (2005) The use of nonnatural nucleotides to probe the contributions of shape complementarity and π-electron surface area during DNA polymerization. *Biochemistry 44*, 13101–13110.
22. Zhang, X., Donnelly, A., Lee, I., and Berdis, A. J. (2006) Rational attempts to optimize non-natural nucleotides for selective incorporation opposite an abasic site. *Biochemistry 45*, 13293–13303.
23. Vineyard, D., Zhang, X., Donnelly, A., Lee, I., and Berdis, A. J. (2007) Optimization of non-natural nucleotides for selective incorporation opposite damaged DNA. *Org. Biomol. Chem. 5*, 3623–3630.
24. Eger, B. T., Kuchta, R. D., Carroll, S. S., Benkovic, P. A., Dahlberg, M. E., Joyce, C. M., and Benkovic, S. J. (1991) Mechanism of DNA replication fidelity for three mutants of DNA polymerase I: Klenow fragment KF(exo+), KF(polA5), and KF(exo-). *Biochemistry 30*, 1441–1448.
25. Berdis, A. J. (2001) Dynamics of translesion DNA synthesis catalyzed by the bacteriophage T4 exonuclease-deficient DNA polymerase. *Biochemistry 40*, 7180–7191.
26. Reineks, E. Z., and Berdis, A. J. (2004) Evaluating the contribution of base stacking during translesion DNA replication. *Biochemistry 43*, 393–404.
27. Loakes, D., Brown, D. M., Linde, S., and Hill, F. (1995) 3-Nitropyrrole and 5-nitroindole as universal bases in primers for DNA sequencing and PCR. *Nucleic Acids Res. 23*, 2361–2366.
28. Loakes, D., and Brown, D. M. (1994) 5-Nitroindole as an universal base analogue. *Nucleic Acids Res. 22*, 4039–4043.
29. Devadoss, B., Lee, I., and Berdis, A. J. (2007) Enhancing the "A-rule" of translesion DNA synthesis: Promutagenic DNA synthesis using modified nucleoside triphosphates. *Biochemistry 46*, 13752–13761.
30. Copeland, R. A. (2000) Enzymes: A practical introduction to structure, mechanism, and data analysis, 2nd ed., Wiley, New York.
31. Sintim, H. O., and Kool, E. T. (2006) Enhanced base pairing and replication efficiency of thiothymidines, expanded-size variants of thymidine. *J. Am. Chem. Soc. 128*, 396–397.
32. Sintim, H. O., and Kool, E. T. (2006) Remarkable sensitivity to DNA base shape in the DNA polymerase active site. *Angew. Chem., Int. Ed. 45*, 1974–1979.
33. Cook, P. F., and Cleland, W. W. (2007) Enzyme Kinetics and Mechanism, 1st ed., Garland Science, New York.
34. Zhang, X., Lee, I., and Berdis, A. J. (2005) A potential chemotherapeutic strategy for the selective inhibition of promutagenic DNA synthesis by nonnatural nucleotides. *Biochemistry 44*, 13111–13121.
35. Furman, P. A., Painter, G., Wilson, J. E., Cheng, N., and Hopkins, S. (1991) Substrate inhibition of the human immunodeficiency virus type 1 reverse transcriptase. *Proc. Natl. Acad. Sci. U.S.A. 88*, 6013–6017.
36. Kumar, S., Bakhtina, M., and Tsai, M. D. (2008) Altered order of substrate binding by DNA polymerase X from African Swine Fever virus. *Biochemistry 47*, 7875–7887.
37. Magee, W. C., Hostetler, K. Y., and Evans, D. H. (2005) Mechanism of inhibition of vaccinia virus DNA polymerase by cidofovir diphosphate. *Antimicrob. Agents Chemother. 49*, 3153–3162.
38. Johnson, K. A. (1993) Conformational coupling in DNA polymerase fidelity. *Annu. Rev. Biochem. 62*, 685–713.
39. McCulloch, S. D., and Kunkel, T. A. (2008) The fidelity of DNA synthesis by eukaryotic replicative and translesion synthesis polymerases. *Cell Res. 18*, 148–161.
40. Shih, P., Pedersen, L. G., Gibbs, P. R., and Wolfenden, R. (1998) Hydrophobicities of the nucleic acid bases: Distribution coefficients from water to cyclohexane. *J. Mol. Biol. 280*, 421–430.
41. Barsky, D., Kool, E. T., and Colvin, M. E. (1999) Interaction and solvation energies of nonpolar DNA base analogues and their role in polymerase insertion fidelity. *J. Biomol. Struct. Dyn. 16*, 1119–1134.
42. Henry, A. A., and Romesberg, F. E. (2003) Beyond A, C, G and T: Augmenting nature's alphabet. *Curr. Opin. Chem. Biol. 7*, 727–733.
43. Matsuda, S., and Romesberg, F. E. (2004) Optimization of interstrand hydrophobic packing interactions within unnatural DNA base pairs. *J. Am. Chem. Soc. 126*, 14419–14427.
44. Wu, Y., Ogawa, A. K., Berger, M., McMinn, D. L., Schultz, P. G., and Romesberg, F. E. (2000) Efforts toward expansion of the genetic alphabet: Optimization of interbase hydrophobic interactions. *J. Am. Chem. Soc. 122*, 7621–7632.
45. Moran, S., Ren, R. X., and Kool, E. T. (1997) A thymidine triphosphate shape analog lacking Watson-Crick pairing ability is replicated with high sequence selectivity. *Proc. Natl. Acad. Sci. U.S.A. 94*, 10506–10511.
46. McCulloch, S. D., Kokoska, R. J., Chilkova, O., Welch, C. M., Johansson, E., Burgers, P. M., and Kunkel, T. A. (2004) Enzymatic switching for efficient and accurate translesion DNA replication. *Nucleic Acids Res. 32*, 4665–4675.
47. Wong, I., Patel, S. S., and Johnson, K. A. (1991) An induced-fit kinetic mechanism for DNA replication fidelity: Direct measurement by single-turnover kinetics. *Biochemistry 30*, 526–537.
48. Kincaid, K., Beckman, J., Zivkovic, A., Halcomb, R. L., Engels, J. W., and Kuchta, R. D. (2005) Exploration of factors driving incorporation of unnatural dNTPS into DNA by Klenow fragment (DNA polymerase I) and DNA polymerase α. *Nucleic Acids Res. 33*, 2620–2628.
49. Chiaramonte, M., Moore, C. L., Kincaid, K., and Kuchta, R. D. (2003) Facile polymerization of dNTPs bearing unnatural base analogues by DNA polymerase α and Klenow fragment (DNA polymerase I). *Biochemistry 42*, 10472–10481.
50. Matsuda, S., Leconte, A. M., and Romesberg, F. E. (2007) Minor groove hydrogen bonds and the replication of unnatural base pairs. *J. Am. Chem. Soc. 129*, 5551–5557.
51. Morales, J. C., and Kool, E. T. (2000) Functional hydrogen-bonding map of the minor groove binding tracks of six DNA polymerases. *Biochemistry 39*, 12979–12988.

52. Arion, D., and Parniak, M. A. (1999) HIV resistance to zidovudine: The role of pyrophosphorolysis. *Drug Resist. Updates 2*, 91–95.
53. Arion, D., Kaushik, N., McCormick, S., Borkow, G., and Parniak, M. A. (1998) Phenotypic mechanism of HIV-1 resistance to 3′-azido-3′-deoxythymidine (AZT): Increased polymerization processivity and enhanced sensitivity to pyrophosphate of the mutant viral reverse transcriptase. *Biochemistry 37*, 15908–15917.
54. Meyer, P. R., Matsuura, S. E., So, A. G., and Scott, W. A. (1998) Unblocking of chain-terminated primer by HIV-1 reverse transcriptase through a nucleotide-dependent mechanism. *Proc. Natl. Acad. Sci. U.S.A. 95*, 13471–13476.
55. Lee, H., Hanes, J., and Johnson, K. A. (2003) Toxicity of nucleoside analogues used to treat AIDS and the selectivity of the mitochondrial DNA polymerase. *Biochemistry 42*, 14711–14719.
56. Chin, J. W., Cropp, T. A., Chu, S., Meggers, E., and Schultz, P. G. (2003) Progress toward an expanded eukaryotic genetic code. *Chem. Biol. 10*, 511–519.
57. Benner, S. A. (1994) Expanding the genetic lexicon: Incorporating non-standard amino acids into proteins by ribosome-based synthesis. *Trends Biotechnol. 12*, 158–163.
58. Kroutil, L. C., Fery, M. F., Kaboord, B. F., Kunkel, T. A., and Benkovic, S. J. (1998) Effect of accessory proteins on T4 DNA polymerase replication fidelity. *J. Mol. Biol. 278*, 134–146.